Journal of Materials Chemistry C

ROYAL SOCIETY OF CHEMISTRY

COMMUNICATION

View Article Online
View Journal | View Issue

Check for updates

Cite this: J. Mater. Chem. C, 2022, 10, 102

Received 21st October 2021,
Accepted 1st December 2021

DOI: 10.1039/d1tc05077j

rsc.li/materials-c

Open Access Article. Published on 10 December 2021. Downloaded on 2/14/2026 3:47:47 PM. This article is licensed under a Creative Commons Attribution 3.0 Unported Licence.

Implications of gas-barrier properties in realizing the self-recovery of photodegraded $CsPbBr_3$ perovskite nanocrystals†

Ikumi Enomoto, Yoshiki Iso * and Tetsuhiko Isobe *

Fluorescent $CsPbBr_3$ perovskite nanocrystals (NCs) degraded by photoinduced desorption of surface ligands can exhibit self-recovery; however, irreversible oxidative damage from oxygen in the atmosphere must be avoided. In this work, gas-barrier polymer films made of ethylene vinyl alcohol (EVOH) and ethylene vinyl acetate (EVA) copolymers were investigated as sealing materials for $CsPbBr_3$ NC films. The NC film covered with EVOH showed photodegradation with blackening and photoluminescence quenching under light excitation, while self-recovery of the optical properties was observed during dark storage. These phenomena were attributed to the photoinduced desorption of surface ligands (and thus the formation of surface defects) and their re-adsorption, respectively. In contrast, self-recovery did not occur when an EVA film was used. X-ray photoelectron spectroscopy indicated the formation of Pb–O bonds for the EVA-coated film. Thus, EVOH, which has a lower oxygen permeability than EVA, successfully prevented irreversible damage by permeated oxygen. This is an important finding for the reuse or lifetime-extension of $CsPbBr_3$ NCs.

All-inorganic $CsPbX_3$ (X = Cl, Br, or I) perovskite nanocrystals (NCs) exhibit remarkable properties, such as high photoluminescence (PL) quantum yields, narrow emission peaks, tunable emission wavelengths, and higher stabilities against heat and moisture, compared with organic–inorganic $APbX_3$ (A: cation) perovskites.[1,2] Accordingly, $CsPbX_3$ NCs are promising materials for optoelectronic applications such as light-emitting diodes (LEDs),[3–9] wide color gamut displays,[10–12] solar devices,[13–17] lasers,[18–20] photodetectors,[21–23] anti-counterfeiting agents,[24–26] and photocatalysts.[27,28] Although the toxic lead in $CsPbX_3$ NCs is a concern in terms of commercialization, the current limit for lead (1000 ppm by weight) in the most recent Restriction of Hazardous Substances (RoHS) guidelines is not as severe as that for cadmium (100 ppm by weight), which is widely used in CdSe quantum dots.[29]

However, the application scope of $CsPbX_3$ NCs is restricted owing to their instability under light irradiation.[30,31] The photodegradation of the NCs is caused by changes in the adsorption states of surface ligands.[32] The interactions between surface ligands and the NC surface are weak and dynamic,[33] leading to their frequent desorption and the formation of surface defects and NC aggregation. When the repulsive forces between dispersed particles due to steric hindrance by surface ligands are lost, the van der Waals forces between the NCs cause aggregation.[34] Furthermore, NC surfaces exposed to the atmosphere are degraded by oxygen as follows:[35]

$$2CsPbBr_3 \bullet H_2O + \frac{1}{2}O_2 + CO_2 \rightarrow 2CsBr + PbCO_3 + Pb(OH)_2 + 2HBr + Br_2 \quad (1)$$

$$Pb(OH)_2 \rightarrow PbO + H_2O \quad (2)$$

In recent years, there have been numerous studies on improving the stability of such NCs under light irradiation by various strategies,[36] such as B-site doping (for ABX_3 perovskites),[37,38] repairing surface traps,[39,40] forming core–shell structures,[41] and matrix encapsulation.[24]

Although significant improvements in photostability have been reported, the PL intensity is not necessarily maintained, particularly when the irradiation intensity is enhanced or prolonged. As a novel strategy, the PL recovery of $CsPbBr_3$ NCs to their initial state after photodegradation should enable their long-term use. The present authors previously reported that, after significant photodegradation by light excitation, solid $CsPbBr_3$ NCs sealed with a glass plate exhibit complete self-recovery of PL properties.[42] In that study, the PL intensity of the NCs decreased to ~20% of the initial intensity under 72 h blue LED irradiation, but then spontaneously increased to 108% upon subsequent dark storage for 2400 h. The solid sample changed from yellow to black during irradiation owing to photoinduced desorption of the surface ligands, but the

Department of Applied Chemistry, Faculty of Science and Technology, Keio University, 3-14-1 Hiyoshi, Kohoku-ku, Yokohama 223-8522, Japan. E-mail: iso@applc.keio.ac.jp, isobe@applc.keio.ac.jp; Fax: +81 45 566 1551; Tel: +81 45 566 1558, +81 45 566 1554

† Electronic supplementary information (ESI) available. See DOI: 10.1039/d1tc05077j

This journal is © The Royal Society of Chemistry 2022

Open Access Article. Published on 10 December 2021. Downloaded on 2/14/2026 3:47:47 PM.
This article is licensed under a Creative Commons Attribution 3.0 Unported Licence.

yellow color was restored after dark storage. We concluded that self-recovery occurs when the desorbed surface ligands are re-adsorbed during dark storage.

Since the self-recovery phenomenon of $CsPbBr_3$ NCs did not occur when the NCs were exposed to air, it was necessary to seal the NCs with a sufficiently thick glass plate. However, in terms of device application scope, using a resin that is easier to mold and more flexible than glass is highly desirable.

In this work, the ethylene vinyl acetate (EVA) copolymer, which is widely used as an encapsulant in solar devices owing to its excellent weather resistance, and the ethylene vinyl alcohol (EVOH) copolymer, which has excellent gas-barrier properties, were used as sealing materials to evaluate their effects on the photodegradation and self-recovery of $CsPbBr_3$ NC films. Film samples of $CsPbBr_3$ NCs with oleic acid and oleylamine as surface ligands were prepared and the effects of the different sealing materials were evaluated by investigating the changes in the film's crystal structure, particle morphology, and optical properties upon degradation by light excitation and subsequent dark storage at 25 °C and 60% relative humidity.

The details of the experimental methods and conditions are given in the ESI.† X-ray diffraction (XRD) analysis revealed that the sample is obtained as cubic $CsPbBr_3$ NCs (Fig. S3, ESI†).

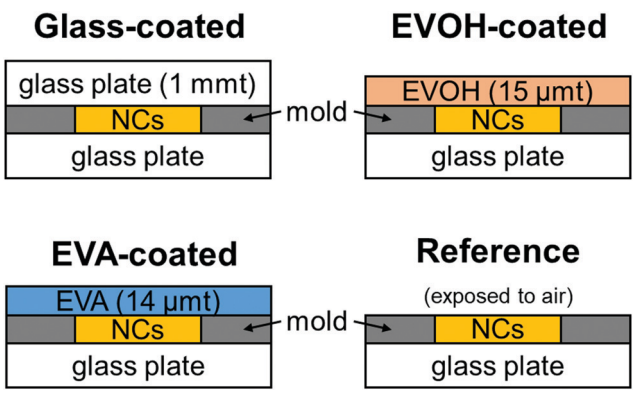

Fig. 1 Schematics of the cross-sectional structure of the $CsPbBr_3$ NC films prepared in this study.

From the transmission electron microscopy (TEM) images (Fig. S4, ESI†), it can be observed that the average particle size of the NCs is 8.8 ± 1.4 nm. The UV-vis absorption and PL spectra of the as-prepared NCs dispersed in toluene show an absorption edge at ~520 nm and an emission peak at 514.4 nm (Fig. S5(a), ESI†). The bandgap estimated from the Tauc plot is 2.39 eV (Fig. S5(b), ESI†), which is larger than the bandgap of cubic $CsPbBr_3$ (~2.3 eV) owing to the quantum size effect.[1]

The properties of the prepared $CsPbBr_3$ NC films as illustrated in Fig. 1 were evaluated during continuous irradiation with 468 nm blue LED light for 72 h and subsequent 168 h dark storage. Fig. 2 shows the appearance of the $CsPbBr_3$ NC films before and after irradiation and storage in the dark. The glass-coated film changes from yellow to black during 72 h irradiation. Correspondingly, its UV-vis absorbance (Fig. 3) increases over the entire wavelength range measured. However, the film regains its yellow color and initial absorbance profile almost completely upon subsequent 168 h dark storage. Similar changes are also observed for the EVOH-coated film. These color changes are attributed to the photoinduced desorption and readsorption of surface ligands on the NCs.[42]

Conversely, the EVA-coated film changes from yellow to orange, as also observed for the reference film, which is exposed to ambient air. The film cannot recover its color, even upon subsequent dark storage for 168 h. The UV-vis spectra of the reference and EVA-coated films also exhibit similar changes during irradiation and dark storage.

Fig. 4 shows the changes in the PL spectra and corresponding PL peak intensities for the films. The intensities for all the samples decrease to 25–50% of the initial values during 72 h irradiation. However, upon 168 h dark storage, the glass- and EVOH-coated films recover their PL intensities to 102% and 77%, respectively. In contrast, the EVA-coated film and reference sample do not exhibit PL self-recovery. It should be noted that the shoulder peak at a longer wavelength could be explained by the photon recycling effect.[43] Such a shoulder peak was not observed for the blackened samples by irradiation for 72 h because the photon recycling effect seems to be reduced by the increased nonradiative relaxation.[44]

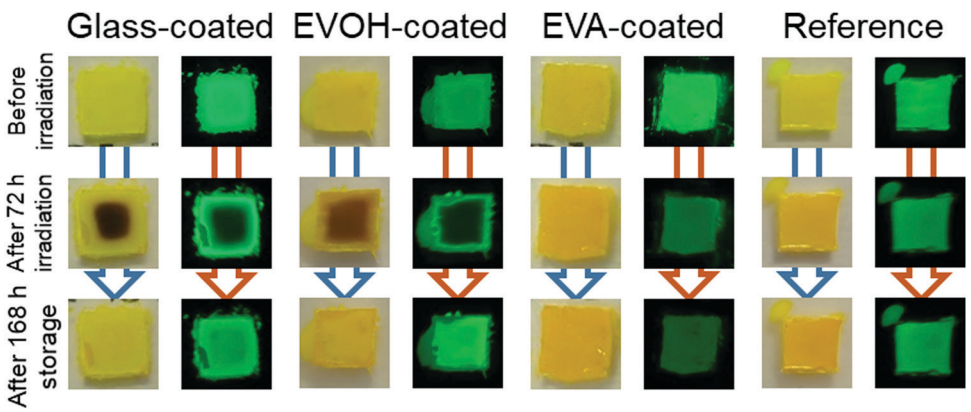

Fig. 2 Images of the $CsPbBr_3$ NC films before and after 72 h irradiation and after subsequent 168 h dark storage. Captured under (left) white light and (right) 365 nm UV light.

Open Access Article. Published on 10 December 2021. Downloaded on 2/14/2026 3:47:47 PM.
This article is licensed under a Creative Commons Attribution 3.0 Unported Licence.

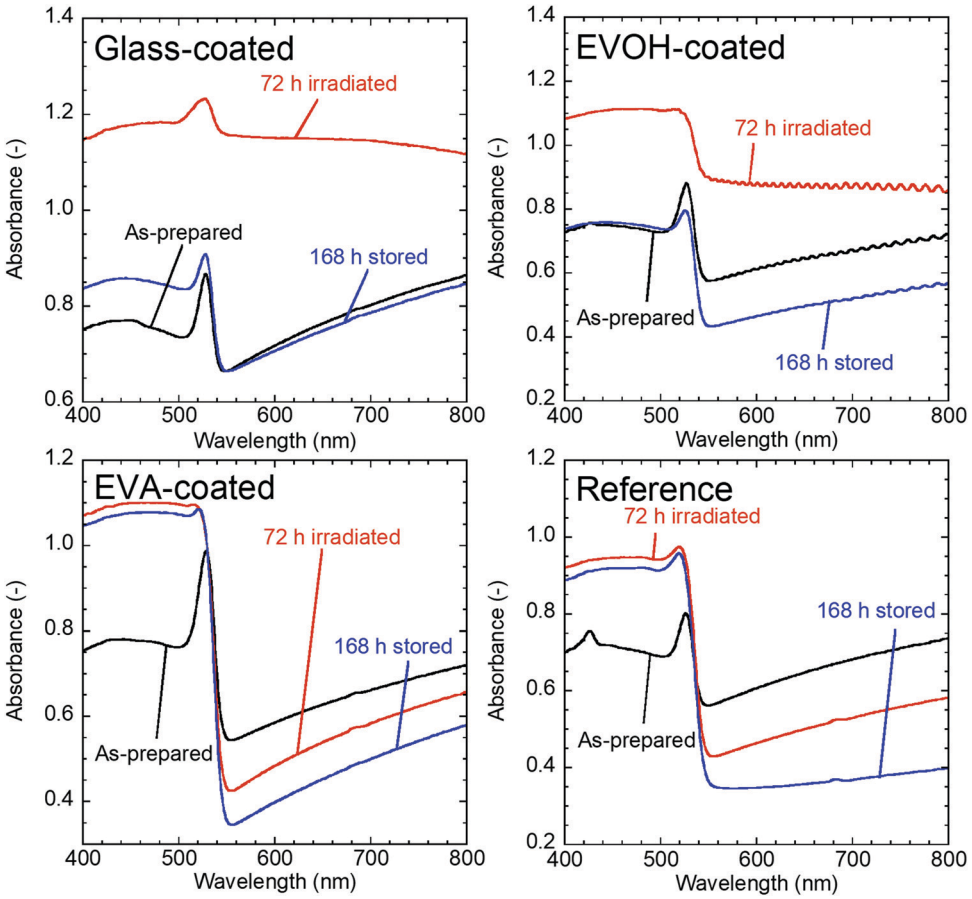

Fig. 3 UV-vis spectra of $CsPbBr_3$ NC films before and after 72 h irradiation and after subsequent 168 h dark storage.

PL decay curves were measured to determine PL lifetimes (see Fig. S6 and Table S1, ESI†). The average PL lifetime for the EVOH-coated film decreases from 27.8 to 11.1 ns upon 72 h irradiation, indicating PL quenching by non-radiative transitions through defects formed under irradiation. According to our previous study, the surface defects presumed to be the cause of sample blackening are generated by the photoinduced desorption of surface ligands adsorbed on the NCs.[42] Upon subsequent 168 h storage in the dark, the average PL lifetime of the EVOH-coated film increases to 29.9 ns, indicating a decrease in the non-radiative transition rate. Therefore, the recovery of absorbance and PL intensity mentioned above is attributed to the reduction of surface defects by readsorption of the desorbed surface ligands. However, the PL decay curves and the corresponding PL lifetimes of the EVA-coated film do not exhibit similar trends. This cannot be explained in terms of the photoinduced desorption and readsorption of surface ligands. Accordingly, other degradation mechanisms should be investigated in future studies.

The TEM observation (Fig. S7, ESI†) revealed that the average particle size for the glass-coated film increases from 8.8 ± 1.4 nm to 10.0 ± 1.9 nm upon 72 h irradiation and remains at 10.3 ± 2.6 nm upon subsequent 168 h dark storage. Similar increases in particle size are observed for the other samples.

These increases in primary particle size can be explained by the following two mechanisms: (i) agglomeration of NCs through contact between the crystal surfaces exposed by desorption of the surface ligands and (ii) crystal growth caused by ion supply to the exposed crystal surface, probably through ionic transport in residual oleic acid and oleylamine molecules that chelate to free metal cations and halide anions in the NC material collected by centrifugation. After light irradiation, the average particle size does not increase because of readsorption of the surface ligands.

XRD analysis was performed to evaluate changes in the crystal structure for the $CsPbBr_3$ NC films upon continuous irradiation (Fig. S8, ESI†). The XRD patterns of all the samples do not change upon 72 h irradiation, revealing that the cubic $CsPbBr_3$ structure is maintained. According to the TEM and XRD analyses, morphology and crystal structure are not related to photodegradation and self-recovery. Therefore, the observed blackening and self-recovery are attributed to reversible photoinduced desorption and readsorption of surface ligands.[42] However, the irreversible degradation without blackening observed for the EVA-coated film and reference sample require further explanation.

X-ray photoelectron spectroscopy (XPS) analysis was performed to investigate the oxidation state of the NCs. The wide-scan XPS spectrum of the as-prepared NCs shown in

 This journal is © The Royal Society of Chemistry 2022

Open Access Article. Published on 10 December 2021. Downloaded on 2/14/2026 3:47:47 PM.
This article is licensed under a Creative Commons Attribution 3.0 Unported Licence.

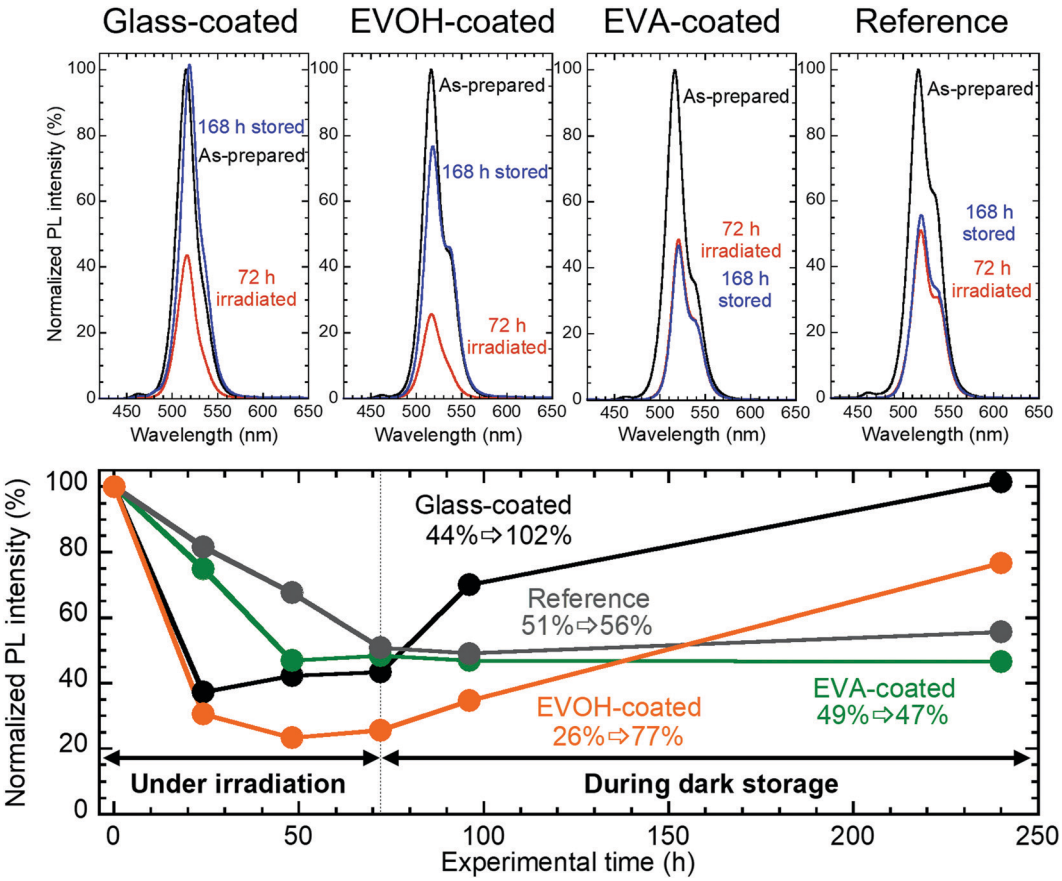

Fig. 4 PL spectra and the corresponding PL peak intensities for $CsPbBr_3$ NC films before and after 72 h irradiation and after subsequent 168 h dark storage. λ_{ex} = 400 nm.

Fig. 5(a) reveals the presence of Cs, Pb, and Br.[45] In our previous work, the Pb $4f_{5/2}$ and $4f_{7/2}$ peaks for $CsPbBr_3$ NCs exposed to ambient air under blue LED irradiation shifted to lower energies due to oxidation by oxygen, whereas the NCs sealed by a glass plate maintained the peak positions after the same irradiation.[44] The peak shifts were attributed to the appearance of the Pb–O peaks at lower energies compared to the Pb–Br peaks; therefore, the changes in the Pb 4f peaks for the EVOH- and EVA-coated films upon 72 h irradiation and subsequent 168 h storage in the dark were investigated (Fig. 5(b)). The Pb $4f_{5/2}$ and $4f_{7/2}$ peaks for the EVOH-coated film appear at 143.1 and 138.3 eV, respectively. These binding energies are attributed to Pb–Br bonds.[34,44] Conversely, both Pb 4f peaks for the EVA-coated film shift to lower energies at 142.9 and 138.0 eV, respectively, after 72 h irradiation. This shift was also observed after subsequent 168 h storage in the dark. According to the peak deconvolutions (see Fig. S9, ESI†), Pb–O peaks appeared at lower binding energies of 142.8 and 137.9 eV than the Pb–Br peaks at 143.1 and 138.3 eV,[35,44] indicating oxidation of $CsPbBr_3$ by oxygen permeated through the EVA film during irradiation. It should be noted that oxidation should occur only near the surface of the NCs because no byproduct is detected by XRD analysis. The irreversible degradation of the EVA-coated film can be explained by oxidation of the exposed surface of NCs. Oxygen that permeated through the EVA film oxidizes the NC surface owing to the loss of surface ligands by photoinduced desorption. This irreversible chemical reaction prevents the recovery of the UV-vis absorption and PL properties for the EVA-coated film and reference sample. The oxidized surface phase might prevent significant decrease in the PL lifetime under irradiation (Fig. S6 and Table S1, ESI†) by passivating the inner fluorescent $CsPbBr_3$ phase, whereas its absorption of excitation light causes the deterioration of PL intensity. In contrast, the EVOH-coated film is not oxidized because of the excellent gas-barrier ability of the EVOH film. The oxygen permeability coefficient of the EVOH film at a relative humidity of 60% and 1 atm is estimated to be $\sim$0.008 mL mm $(m^2$ day atm$)^{-1}$,[46] and this value is much lower than that of the EVA film (145.8 mL mm $(m^2$ day atm$)^{-1}$).[47] Therefore, the self-recovery of $CsPbBr_3$ NCs can be realized by a suitable resin film instead of a glass plate.

In this work, the effects of coating with EVA and EVOH films on the photodegradation and self-recovery of $CsPbBr_3$ NC films were evaluated. The EVOH-coated film shows blackening and a decrease in PL intensity under light excitation, followed by recovery upon subsequent dark storage, similar to the glass-coated film. These phenomena are attributed to the photoinduced desorption of surface ligands, which induces the formation of surface defects and their readsorption after irradiation. Conversely, the EVA-coated film shows irreversible photodegradation similar to that observed for the reference sample, which is exposed to

Open Access Article. Published on 10 December 2021. Downloaded on 2/14/2026 3:47:47 PM.
This article is licensed under a Creative Commons Attribution 3.0 Unported Licence.

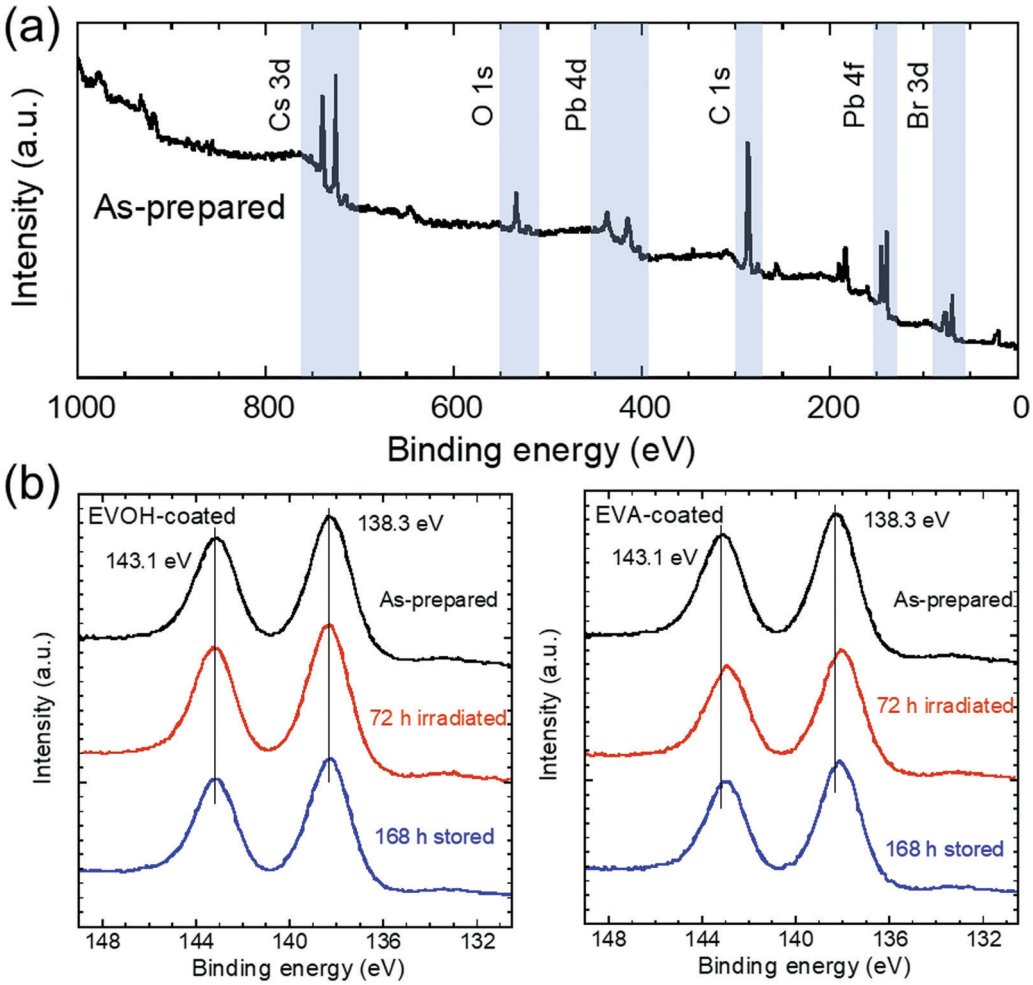

Fig. 5 (a) XPS spectrum of the as-prepared $CsPbBr_3$ NC film. (b) Pb 4f peaks after 72 h irradiation and subsequent 168 h dark storage.

ambient air. This irreversible degradation cannot be explained in terms of the reversible desorption and readsorption of surface ligands. In the XPS spectra of the EVOH-coated film, Pb 4f peaks assigned to Pb–Br bonding are observed. Conversely, peaks attributed to Pb–O bonding are observed for the EVA-coated film, revealing that oxygen permeates through the EVA film. The EVOH film has a much lower oxygen permeability coefficient than the EVA film, preventing irreversible oxidation. Therefore, the self-recovery of photodegraded $CsPbBr_3$ NCs can be realized by the use of a suitable resin film material, such as EVOH. These are important findings and will have far-reaching implications for the application of $CsPbBr_3$ self-recovery as a means to realize its reuse or lifetime-extension for next-generation optoelectronic devices.

Conflicts of interest

There are no conflicts to declare.

Acknowledgements

This work was supported by the Hosokawa Powder Technology Foundation, the Nippon Sheet Glass Foundation for Materials Science and Engineering, the Mizuho Foundation for the Promotion of Sciences, and JSPS KAKENHI Grant Number JP20K15131.

References

1 L. Protesescu, S. Yakunin, M. I. Bodnarchuk, F. Krieg, R. Caputo, C. H. Hendon, R. X. Yang, A. Walsh and M. V. Kovalenko, *Nano Lett.*, 2015, **15**, 3692–3696.
2 J. Song, J. Li, X. Li, L. Xu, Y. Dong and H. Zeng, *Adv. Mater.*, 2015, **27**, 7162–7167.
3 C. Chen, D. Li, Y. Wu, C. Chen, Z. G. Zhu, W. Y. Shih and W. H. Shih, *Nanotechnology*, 2020, **31**, 225602.
4 M. Cao, Y. Xu, P. Li, Q. Zhong, D. Yang and Q. Zhang, *J. Mater. Chem. C*, 2019, **7**, 14412–14440.
5 H. Wang, X. Zhang, Q. Wu, F. Cao, D. Yang, Y. Shang, Z. Ning, W. Zhang, W. Zheng, Y. Yan, S. V. Kershaw, L. Zhang, A. L. Rogach and X. Yang, *Nat. Commun.*, 2019, **10**, 665.
6 J. S. Yao, J. Ge, K. H. Wang, G. Zhang, B. S. Zhu, C. Chen, Q. Zhang, Y. Luo, S. H. Yu and H. Bin Yao, *J. Am. Chem. Soc.*, 2019, **141**, 2069–2079.

 This journal is © The Royal Society of Chemistry 2022

Open Access Article. Published on 10 December 2021. Downloaded on 2/14/2026 3:47:47 PM.
This article is licensed under a Creative Commons Attribution 3.0 Unported Licence.

7 J. H. Park, A. Y. Lee, J. C. Yu, Y. S. Nam, Y. Choi, J. Park and M. H. Song, *ACS Appl. Mater. Interfaces*, 2019, **11**, 8428–8435.
8 W. Yang, F. Gao, Y. Qiu, W. Liu, H. Xu, L. Yang and Y. Liu, *Adv. Opt. Mater.*, 2019, **7**, 1900546.
9 P. Cao, B. Yang, F. Zheng, L. Wang and J. Zou, *Ceram. Int.*, 2020, **46**, 3882–3888.
10 J. Tong, J. Wu, W. Shen, Y. Zhang, Y. Liu, T. Zhang, S. Nie and Z. Deng, *ACS Appl. Mater. Interfaces*, 2019, **11**, 9317–9325.
11 Y. Yin, Z. Hu, M. U. Ali, M. Duan, L. Gao, M. Liu, W. Peng, J. Geng, S. Pan, Y. Wu, J. Hou, J. Fan, D. Li, X. Zhang and H. Meng, *Adv. Mater. Technol.*, 2020, **5**, 2000251.
12 S. Mei, B. Yang, X. Wei, H. Dai, Z. Chen, Z. Cui, G. Zhang, F. Xie, W. Zhang and R. Guo, *Nanomaterials*, 2019, **9**, 832.
13 F. Wang, M. Yang, S. Ji, L. Yang, J. Zhao, H. Liu, Y. Sui, Y. Sun, J. Yang and X. Zhang, *J. Power Sources*, 2018, **395**, 85–91.
14 J. Duan, Y. Wang, X. Yang and Q. Tang, *Angew. Chem., Int. Ed.*, 2020, **59**, 4391–4395.
15 W. Zhang, X. Liu, B. He, Z. Gong, J. Zhu, Y. Ding, H. Chen and Q. Tang, *ACS Appl. Mater. Interfaces*, 2020, **12**, 4540–4548.
16 X. Liu, X. Tan, Z. Liu, H. Ye, B. Sun, T. Shi, Z. Tang and G. Liao, *Nano Energy*, 2019, **56**, 184–195.
17 Y. Gao, Y. Wu, H. Lu, C. Chen, Y. Liu, X. Bai, L. Yang, W. W. Yu, Q. Dai and Y. Zhang, *Nano Energy*, 2019, **59**, 517–526.
18 Q. Zhang, R. Su, X. Liu, J. Xing, T. C. Sum and Q. Xiong, *Adv. Funct. Mater.*, 2016, **26**, 6238–6245.
19 Z. Liu, Q. Shang, C. Li, L. Zhao, Y. Gao, Q. Li, J. Chen, S. Zhang, X. Liu, Y. Fu and Q. Zhang, *Appl. Phys. Lett.*, 2019, **114**, 101902.
20 S. Yuan, D. Chen, X. Li, J. Zhong and X. Xu, *ACS Appl. Mater. Interfaces*, 2018, **10**, 18918–18926.
21 P. Ramasamy, D. H. Lim, B. Kim, S. H. Lee, M. S. Lee and J. S. Lee, *Chem. Commun.*, 2016, **52**, 2067–2070.
22 J. Zeng, H. Zhou, R. Liu and H. Wang, *Sci. China Mater.*, 2019, **62**, 65–73.
23 J. Zeng, X. Li, Y. Wu, D. Yang, Z. Sun, Z. Song, H. Wang and H. Zeng, *Adv. Funct. Mater.*, 2018, **28**, 1804394.
24 F. Zhang, Z. Shi, S. Li, Z. Ma, Y. Li, L. Wang, D. Wu, Y. Tian, G. Du, X. Li and C. Shan, *ACS Appl. Mater. Interfaces*, 2019, **11**, 28013–28022.
25 X. Yu, L. Wu, D. Yang, M. Cao, X. Fan, H. Lin, Q. Zhong, Y. Xu and Q. Zhang, *Angew. Chem., Int. Ed.*, 2020, **59**, 14527–14532.
26 Y. Liu, F. Li, L. Qiu, K. Yang, Q. Li, X. Zheng, H. Hu, T. Guo, C. Wu and T. W. Kim, *ACS Nano*, 2019, **13**, 2042–2049.
27 Y. W. Liu, S. H. Guo, S. Q. You, C. Y. Sun, X. L. Wang, L. Zhao and Z. M. Su, *Nanotechnology*, 2020, **31**, 215605.
28 Y. F. Xu, M. Z. Yang, B. X. Chen, X. D. Wang, H. Y. Chen, D. Bin Kuang and C. Y. Su, *J. Am. Chem. Soc.*, 2017, **139**, 5660–5663.
29 Q. A. Akkerman, G. Rainò, M. V. Kovalenko and L. Manna, *Nat. Mater.*, 2018, **17**, 394–405.
30 J. Chen, D. Liu, M. J. Al-Marri, L. Nuuttila, H. Lehtivuori and K. Zheng, *Sci. China Mater.*, 2016, **59**, 719–727.
31 H. Hu, L. Wu, Y. Tan, Q. Zhong, M. Chen, Y. Qiu, D. Yang, B. Sun, Q. Zhang and Y. Yin, *J. Am. Chem. Soc.*, 2018, **140**, 406–412.
32 T. Kosugi, Y. Iso and T. Isobe, *Chem. Lett.*, 2019, **48**, 349–352.
33 Y. Wang, X. Li, S. Sreejith, F. Cao, Z. Wang, M. C. Stuparu, H. Zeng and H. Sun, *Adv. Mater.*, 2016, **28**, 10637–10643.
34 S. Huang, Z. Li, B. Wang, N. Zhu, C. Zhang, L. Kong, Q. Zhang, A. Shan and L. Li, *ACS Appl. Mater. Interfaces*, 2017, **9**, 7249–7258.
35 J. Li, L. Wang, X. Yuan, B. Bo, H. Li, J. Zhao and X. Gao, *Mater. Res. Bull.*, 2018, **102**, 86–91.
36 Y. Wei, Z. Cheng and J. Lin, *Chem. Soc. Rev.*, 2019, **48**, 310–350.
37 S. Zou, Y. Liu, J. Li, C. Liu, R. Feng, F. Jiang, Y. Li, J. Song, H. Zeng, M. Hong and X. Chen, *J. Am. Chem. Soc.*, 2017, **139**, 11443–11450.
38 H. Liu, Z. Wu, J. Shao, D. Yao, H. Gao, Y. Liu, W. Yu, H. Zhang and B. Yang, *ACS Nano*, 2017, **11**, 2239–2247.
39 B. A. Koscher, J. K. Swabeck, N. D. Bronstein and A. P. Alivisatos, *J. Am. Chem. Soc.*, 2017, **139**, 6566–6569.
40 H. Li, Y. Qian, X. Xing, J. Zhu, X. Huang, Q. Jing, W. Zhang, C. Zhang and Z. Lu, *J. Phys. Chem. C*, 2018, **122**, 12994–13000.
41 Z. J. Li, E. Hofman, J. Li, A. H. Davis, C. H. Tung, L. Z. Wu and W. Zheng, *Adv. Funct. Mater.*, 2018, **28**, 1704288.
42 K. Kidokoro, Y. Iso and T. Isobe, *J. Mater. Chem. C*, 2019, **7**, 8546–8550.
43 Z. Gan, X. Wen, W. Chen, C. Zhou, S. Yang, G. Cao, K. P. Ghiggino, H. Zhang and B. Jia, *Adv. Energy Mater.*, 2019, **9**, 1900185.
44 K. Miyashita, K. Kidokoro, Y. Iso and T. Isobe, *ACS Appl. Nano Mater.*, 2021, **4**, 12600–12608.
45 K. Xu, E. T. Vickers, B. Luo, Q. Wang, A. C. Allen, H. Wang, V. Cherrette, X. Li and J. Z. Zhang, *Sol. Energy Mater. Sol. Cells*, 2020, **208**, 110341.
46 Z. Zhang, I. J. Britt and M. A. Tung, *J. Appl. Polym. Sci.*, 2001, **82**, 1866–1872.
47 Y. Zhong, D. Janes, Y. Zheng, M. Hetzer and D. De Kee, *Polym. Eng. Sci.*, 2007, **47**, 1101–1107.